Lipopolysaccharide interaction is decisive for the activity of the antimicrobial peptide NK-2 against Escherichia coli and Proteus mirabilis

Malte U. Hammer, Annemarie Brauser, Claudia Olak, Gerald Brezesinski, Torsten Goldmann, Thomas Gutsmann, Jörg Andrä

Lipopolysaccharide interaction is decisive for the activity of the antimicrobial peptide NK-2 against *Escherichia coli* and *Proteus mirabilis*[†]

Malte U. Hammer[*†], Annemarie Brauser[*], Claudia Olak[‡], Gerald Brezesinski[‡], Torsten Goldmann[*], Thomas Gutsmann[*], and Jörg Andrä[*1]

[*]Research Center Borstel, Leibniz-Center for Medicine and Biosciences, Parkallee 10, D-23845 Borstel, Germany; [†]present address: UCSB, Santa Barbara, CA; [‡]Max-Planck-Institute of Colloids and Interfaces, Am Mühlenberg 1, D-14476 Potsdam, Germany

[1]**Corresponding author:** Jörg Andrä, Division of Biophysics, Research Center Borstel, Leibniz-Center for Medicine and Biosciences, Parkallee 10, D-23845 Borstel, Germany, Tel. 49-4537-188280; fax 49-4537-188632; Email: jandrae@fz-borstel.de

Short title: Lipopolysaccharide interaction of antimicrobial peptides

Abbreviations: AFM, atomic force microscopy; AMP, antimicrobial peptide; CD, circular dichroism; CFU, colony forming unit; TEM, transmission electron microscopy; FRET, Förster resonance energy transfer; LPS, lipopolysaccharide; MIC, minimal inhibitory concentration; MBC, minimal bactericidal concentration; PE, phosphatidylethanolamine; PG, phosphatidylglycerol; NBD, N-(7-nitrobenz-2-oxa-1,3-diazol-4yl); Rh, rhodamin; SAW, surface acoustic wave, TFE, trifluoroethanol.

SYNOPSIS

Phosphatidylglycerol is a widely used mimetic to study the effects of antimicrobial peptides (AMPs) on the bacterial cytoplasmic membrane. It turned out, however, that the antibacterial activities of novel NK-2-derived AMPs could not sufficiently explained by using this simple model system. Since the lipopolysaccharide (LPS) containing outer membrane is the first barrier of Gram-negative bacteria, here we investigated interactions of NK-2 and a shortened variant thereof with viable *Escherichia coli* WBB01 and *Proteus mirabilis* R45, and with model membranes composed of LPS isolated from these two strains. Differences in net charge and charge distribution of the two LPS have been made responsible for the differential sensitivity of the respective bacteria to other AMPs. As imaged by transmission electron microscopy (TEM) and atomic force microscopy (AFM), NK-2-mediated killing of these bacteria was corroborated by structural alterations of the outer and inner membranes, the release of *E. coli* cytoplasma, and the formation of unique fibrous structures inside *P. mirabilis*, suggesting distinct and novel intracellular targets. NK-2 bound to and intercalated into LPS bilayers, and eventually induced the formation of transient, heterogeneous lesions in planar lipid bilayers. However, the discriminative activity of NK-2 against the two bacterial strains was independent from membrane intercalation and lesion formation, which both were indistinguishable for the two LPS. Instead, differences in activity originated from the LPS binding step, which could be demonstrated by NK-2 attachment to intact bacteria, and to solid-supported LPS bilayers on a surface acoustic wave biosensor.

Keywords: antimicrobial peptide, atomic force microscopy, biosensor, endotoxin, membrane permeabilization, NK-lysin

INTRODUCTION

The emergence of a rising number of bacterial strains resistant against common antibiotics has urged the search for potent alternatives [1, 2]. Over the last decades natural antimicrobial peptides (AMPs) and derivatives thereof have attracted the interest of researchers and pharmacologists [3, 4]. AMPs are effective against bacteria, including multi-resistant strains, prevent biofilm formation [5], and thus have gained high interest as lead structures for new anti-infectives. To adopt these compounds for clinical applications it is of utmost importance to understand their mode of action on a molecular level. Cationicity and amphipathicity enable interaction with the cell wall of bacteria, and a dysfunction of this barrier as a direct consequence of peptide membrane interaction has been widely accepted as important step in peptide-mediated killing of bacteria [6-8]. This eventually results either in direct killing of bacteria or allows the uptake of the antibiotic peptide into the bacteria [9, 10]. The molecular basis behind this mechanism, however, is still a matter of debate and far from being set.

We selected the peptide NK-2 [11], representing the cationic core region of NK–lysin, as a model compound to understand the molecular principles of bacterial killing and membrane interaction of AMPs. NK-lysin has been isolated originally from porcine NK cells. It exhibits antibacterial as well as tumourolytic activities [12]. Homologue proteins have been described in human (granulysin [13]), pathogenic amoeba (amoebapores [14]), and other species [15-17]. They are all membrane-interacting proteins [18] and belong to the saposin-like protein family (SAPLIP) [19], which is characterized by a common α-helical fold stabilized by three disulfide bridges [20, 21]. Structure-function analysis of amoebapores showed that its central α-helical region is the key factor for membrane interaction [22, 23]. Inspired by the homology of amoebapore to NK-lysin [24], we synthesized the respective α-helical fragment of NK-lysin, termed NK-2, and investigated its biological activities and membrane-interaction properties.

The peptide NK-2 consists of 27 amino acid residues with an overall positive net charge due to arginine and lysine residues. It adopts an amphipathic, α-helical secondary structure in TFE and upon phospholipid interaction [11, 25-27]. NK-2 kills bacteria [26], fungi [11], parasites [28, 29], as well as certain cancer cells [30]. Additionally it is an effective neutralizing agent of bacterial endotoxin (lipopolysaccharide, LPS) [31]. In contrast to this, human erythrocytes [11], glioblastoma cells [28], and primary lymphocytes [30] have been found to be protected against cytotoxic NK-2 effects. Because of this selectivity for bacteria over normal human cells, NK-2 is a potential ´peptide antibiotic´ for therapeutic usage.

The selectivity of NK-2 could be assigned to differences in the membrane phospholipid composition of the target cells [25, 26, 30]. Whereas bacterial membranes are characterized by a substantial amount of negatively charged lipids, e.g. LPS in the outer membrane and phosphatidylglycerol (PG) and cardiolipin in the cytoplasmic membrane, the outer layer of the plasma membrane of human cells consists of the zwitterionic phosphatidylcholine (PC) and sphingomyelin and lacks anionic phospholipids [32]. NK-2 has been shown to bind to negatively charged phosholipid model membranes and to permeabilize them, but not to zwitterionic ones. However, neither conductivity, voltage dependency, nor life time of NK-2-induced lesions in phosholipid membranes or any other membranes have been characterized yet.

In a previous paper we screened the activities of NK-2 and of a set of peptides inspired from the NK-2 sequence against a panel of Gram-negative bacterial strains [26]. Although PG is the main target of NK-2 in membranes mimicking the cytoplasmic bacterial membrane [25, 33], only a qualitative but no quantitative correlation has been found between the antibiotic activity and the degree of peptide intercalation into PG liposomes.

Apparently, in the case of Gram-negative bacteria, the outer layer of the outer membrane is the first barrier against all antibiotic compounds. Described targets for AMPs are the destruction of the cytoplasmic membrane or further intracellular targets [9, 10]. Either way, peptides have to attach to the LPS layer and permeate through the outer membrane to reach their final target [34, 35]. Therefore, the overcome of the LPS containing membrane is crucial for the mode of action of AMPs against Gram-negative bacteria. The lipid matrix of the outer layer of the highly asymmetric outer membrane is composed almost exclusively of the glycolipid LPS, which is considered to be the first target structure for AMPs in the case of Gram-negative bacteria. In particular, the chemical compositions of the LPS carbohydrate chains determine its interaction with NK-2 and lactoferricin-derived peptides [31, 36]. Thus, we extended our studies and dissected the different steps of NK-2 interactions (association, insertion, permeabilization) with artificial membranes composed of LPS and with live bacteria more detailed. We focused on two Gram-negative bacterial strains which exhibit pronounced differences in the susceptibility to various AMPs including the membrane permeabilizing antibiotic polymyxin B. This differential susceptibility could be assigned to variations in the degree of positively charged arabinose attached to phosphate groups of the LPS headgroup and to the Kdo core carbohydrates resulting in differences in net charge and charge distributions of the individual LPS structures [35, 37, 38]. Our working hypothesis is that these structural changes are decisive for differences in the antibiotic action of AMPs as they prevent or reduce the electrostatic attraction of the polycationic AMPs and the anionic LPS. To bridge the gap between the interaction of peptides with bacteria and artificial membranes, we isolated LPS from the bacterial strains we used for the biological assays. This chemically well-defined LPS was used for the reconstitution of biologically relevant model membranes of different complexity: we comprehensively investigated the interaction of NK-2 and its biologically inactive derivative NK11 [26] with LPS aggregates, immobilized LPS bilayers, and non-supported Montal-Mueller asymmetric LPS/phospholipid planar bilayers. Various biophysical techniques, including circular dichroism (CD) spectroscopy, surface acoustic wave (SAW) biosensor, trans-membrane conductivity measurements, and FRET spectroscopy were used to characterize the effects of the used peptides to these reconstituted model membranes. These biophysical studies were complemented by experiments using intact bacteria, which provide information about the direct binding of peptides to bacteria, permeabilization of bacterial membranes, bacterial viability and change of the bacterial morphology upon peptide treatment.

EXPERMIMENTAL

Peptides

NK-2 (KILRGVCKKIMRTFLRRISKDILTGKK-NH_2), NK11 (KISKRILTGKK-NH_2), and melittin (GIGAVLKVLTTGLPALISWIKRKRQQ-NH_2) were synthesized with an amidated C terminus by the Fmoc solid-phase peptide synthesis technique on an automatic peptide synthesizer (model 433 A; Applied Biosystems) as described [31]. NBD-labelled NK-2 was prepared as follows: Peptide coupled to the resin and with protected sidechains was suspended in dimethylformamide, supplemented with trace amounts of pyridine. Then, a 4-fold molar excess of 4-chloro-7-nitro-1,2,3-benzoxadiazole (NBD chloride, Fluka, Germany) was added and the suspension was stirred gently overnight at 20°C. The resin was filtered, washed and the peptide was cleaved from the resin as described above. Polymyxin B was purchased from Sigma Aldrich (Deisenhofen, Germany).

Bacterial strains

All used bacterial strains were LPS rough or deep rough mutants: *Salmonella enterica* (serovar Minnesota) strain R60 (LPS Ra) and strain R595 (LPS Re), *Escherichia coli* strain

WBB01 (LPS Re), and *Proteus mirabilis* strain R45 (LPS Re). Bacteria were grown over night in Luria-Bertani (LB) medium composed of 1% tryptone, 0.5% yeast extract, and 1% NaCl under constant shaking at 37°C and subsequently inoculated in the same medium to reach the mid-exponential phase.

Lipids and reagents

Phospholipids (cardiolipin (bovine heart), L-α-phosphatidylethanolamine (PE, *Escherichia coli*), L-α-phosphatidyl-DL-glycerol (PG, chicken egg)) were purchased from Avanti Polar Lipids (Alabaster, AL, USA). Fluorescently labelled phospholipids N-(7-nitrobenz-2-oxa-1,3-diazol-4yl)-phosphatidylethanolamine (NBD-PE) and N-(lissamine rhodamine B sulfonyl)-phosphatidylethanolamine (Rh-PE) were from Molecular Probes (Eugene, OR, USA). Rough type LPS were extracted by the phenol/chloroform/petrol ether method from bacteria grown at 37°C, purified, and lyophilized [39]. All other chemicals were analytical grade and acquired from Merck (Darmstadt, Germany).

Preparation of LPS aggregates

LPS dispersed in buffer (see respective method) by vortexing, was sonicated in a water bath for 30 min at 60°C. The samples were heated up to 60°C and cooled down to room temperature three or four times. After this cycles, the lipid samples were stored at least 12 h at 4°C before used. The size of the LPS aggregates in water was determined by dynamic light scattering. There are mainly two populations with 72 nm and 256 nm in a ration of 2:1, respectively.

Assay for antibacterial activity

The peptides were dissolved at the desired concentration in assay buffer (20 mM HEPES, pH 7.0 with or without additional 150 mM NaCl), and 180 µl of these solutions were filled in the wells of the first row of a microtiter plate. For a two-fold serially dilution, 90 µl of each peptide solution were transferred to the well in the next row, which was filled with 90 µl buffer before. Subsequently, a suspension of exp-phase bacteria in LB was added (10 µl, containing 10^4 CFU) to the peptide solution (90 µl). The constantly shaken plates were incubated in a wet chamber over night at 37°C. Bacterial growth was monitored by measuring the optical density at 620 nm in a microtiter plate reader (Rainbow, Tecan, Crailsham, Germany). The minimal inhibitory concentration (MIC) was defined as the lowest peptide concentration at which no bacterial growth was measurable. Portions of each well (10 µl) were diluted with buffer and plated out in duplicates on LB-agar plates. After incubation over night at 37°C bacterial colonies were counted. The minimal bactericidal concentration (MBC) was defined as the lowest peptide concentration at which no colony growth was observed. Determination of the time course of bacterial killing was performed in 20 mM HEPES, 150 mM NaCl, pH 7.0 without additional nutrient as described previously in detail [41].

Electron microscopy

Transmission electron microscopy (TEM) was performed as described previously in detail [26]. Bacteria ($5x10^8$ CFU/ml) were incubated with indicated concentrations of NK-2 and NK11 in buffer (20 mM HEPES, 150 mM NaCl, pH 7.0) supplemented with 10% LB medium for 30 min at 37°C. Images shown are representative for the respective sample.

Atomic force microscopy

Bacteria and bacteria/peptide samples as prepared for TEM were placed on mica, excess liquid was removed with filter paper and the bacteria were air dried at room temperature for 24 h. Dried bacteria were rinsed with 3 ml H_2O and imaged with an atomic force microscope in air using a MFP-3D (Asylum Research, Santa Barbara, CA, USA).

Imaging in air was performed with NSG11-B cantilever (k= 5.5 N/m; NT-MDT, Moscow, Russia) in AC (tapping) mode using frequencies of about 150 kHz. The frequency was chosen to result in an amplitude 5% lower than the amplitude at the resonance frequency. The set point was always adjusted to guarantee minimum forces applied to the sample. Further image processing (flattening and plane fitting) was done with the MFP-3D software under IGOR Pro (Lake Oswego, OR, USA). Images shown are representative for the respective sample.

Binding of fluorescently labelled peptide to live bacteria

Exp-phase bacteria were washed in Dulbecco's phosphate buffered saline without Ca^{2+}, pH 7.4 (PBS, Biochrom AG, Berlin, Germany) and adjusted to $5x10^8$ CFU/ml. NBD-NK-2 was added to the bacteria (800 µl, 10 µM final peptide concentration) and the suspension was incubated for 20 min at 37°C. The bacterial suspension was then analyzed with a fluorescence assisted cell sorter (FACS) flow cytometer (FACSCalibur, BD Biosciences, Heidelberg, Germany) with computer-assisted evaluation of data (CellQuest software). Bacteria were selected by Forward Scattered (FSC) and Side Scattered (SSC) signals. Then, we measured the intensity of green fluorescence (FL-1) of 10,000 single bacteria with and without fluorescently labelled peptide NBD-NK-2. By adding the measured fluorescence intensity multiplied with the corresponding number of observed events, we measure the relative amount of bound peptide. To take care of the self-fluorescence of used bacteria, the measured values of bacteria without peptide were subtracted and afterwards normalized to fluorescence intensity of NBD-NK-2 bound to bacteria of *E. coli* strain WBB01. Data presented are the mean of two independent experiments each performed in duplicates.

SYTOX green uptake assay

Bacteria with compromized membranes were detected by monitoring the fluorescence of the DNA-intercalating dye SYTOX Green (Invitrogen, Molecular Probes). Bacteria (*E. coli* strain WBB01) were grown to mid-exponential phase in LB medium and washed twice with and resuspended in 5 mM HEPES, 100 mM NaCl, pH 7.0 at a density of 10^7 CFU/ml. Peptides were diluted in the same buffer and incubated with bacteria ($5x10^5$ CFU) and with 2 µM of the fluorescent dye SYTOX Green in a total volume of 200 µl at 37 °C for 30 min. Permeabilization of the bacterial membranes allows the dye to enter the cytoplasm and to intercalate into the DNA. After incubation, the mixture was diluted 5 times and a fluorescence spectrum of the samples was measured after excitation at 488 nm in acryl cuvettes with a spectrofluorometer (Fluorolog-3, Horiba, USA). Total fluorescence intensity was obtained by curve integration from 504-600 nm. Membrane-permeabilizing activity of the peptides is expressed as percentage of permeabilized bacteria. For spontaneous lysis of the bacteria (0% value), incubation was done in buffer, for maximum permeabilization (100% value), cells were incubated with 0.5% triton x-100 in buffer. Experiments were done at least twice. Data shown represent mean +/- standard deviation.

Surface acoustic wave (SAW) biosensor measurements

Binding of peptides to immobilized lipid bilayers was analyzed using the S-sens K5 biosensor device (Biosensor GmbH, Bonn, Germany). The procedure has been described in detail elsewhere [42]. Note that in contrast to the previously described procedure, here we used a different type of dextran (see below). Functionalization of gold-coated chips (S-sens K5 Biosensor Quartz Chips, Biosensor GmbH, Bonn, Germany) was achieved by epichlorhydrine (Sigma) coupling of dextran (3 mg/ml in 0.1 M NaOH, average molecular mass 400–500 kDa, Sigma) to a self-assembled monolayer of 11-mercapto-1-undecanol (Aldrich), and finally carboxylation of dextran with bromoacetic acid (Sigma). The dry chip was stored until use at 4°C. Measurements were performed at a continuous buffer (5 mM

HEPES, 100 mM KCl, pH 7.0, or, if indicated, 20 mM HEPES, pH 7.0 without or with additional 150 mM NaCl) flow of 20 µl/min at 22°C. By injection of 100 µl poly-L-lysin (PLL, 60 µg/ml, Fluka, Basel, Switzerland) a positively charged layer was formed on top of the negatively charged carboxymethylated-dextran matrix. Formation of a LPS bilayer was done by two consecutive injections of LPS aggregates (180 µl, 100 µM) each followed by 5 min buffer rinse. Peptide injections (= adsorption, 200 µl) were followed by 10 min buffer rinse (= desorption). Peptide binding to the PLL layer was negligible. All injections, but those containing peptide, were performed with an initial burst, a brief increase in flow to 150 µl/min. All binding experiments were performed at least with three independent preparations of LPS aggregates. Representative traces are shown. Phase shift of an acoustic surface wave corresponds roughly to a change in mass loading on the surface and is presented here normalized to the phase shift induced by the formation of the lipid bilayer.

CD spectroscopy

The LPS dispersion was prepared as described above. CD data were acquired with a Jasco J-715 CD spectrophotometer using quartz cuvettes with an optical path length of 0.1 cm. The response was measured from 190 to 300 nm with 0.2 nm step resolution and 1 nm bandwidth at 20°C. The rate was 50 nm/min using a 2 s response time. Each spectrum is a sum of at least four scans to improve the signal-to-noise ratio. All spectra are reported in terms of mean residue molar ellipticity ($[\theta]_R$ = deg cm^2 $dmol^{-1}$). Spectra were collected for samples of 63 µM peptide and 0.1 mM LPS in 10 mM potassium phosphate at pH 7.0 and 20°C.

Förster resonance energy transfer (FRET) spectroscopy

Intercalation of peptides into LPS aggregates was determined in 20 mM HEPES, pH 7.0 or in 20 mM HEPES, 150 mM NaCl, pH 7.0 at 37°C by FRET spectroscopy applied as a probe dilution assay [43]. The peptide was added to LPS aggregates, which were labelled with 1% of the donor NBD-phosphatidylethanolamine (NBD-PE) and 1% of the acceptor Rhodamine-PE. NBD-excitation wavelength was 470 nm. Intercalation was monitored as the increase of the ratio of the donor fluorescence intensity I_D at 531 nm to that of the acceptor intensity I_A at 593 nm (FRET signal) in dependence on time. This ratio depends on the Förster efficiency, therefore a rising value means that the mean distance separation of donor and acceptor dyes is raising.

Preparation of planar bilayers and electrical measurements

Planar bilayers were prepared according to the Montal-Mueller technique [44] as described earlier [45]. Briefly, symmetric and asymmetric bilayers were formed by opposing two lipid monolayers, prepared in separated compartments on aqueous subphases from chloroformic solutions of the lipids, at a small aperture (ca. 150 µm) in a thin teflon septum (thickness 25 µm). The inner leaflet of the outer membrane of Gram-negative bacteria was reconstituted by a phospholipid mixture (PL) consisting of PE, PG, and cardiolipin (molar ratio 81:17:2) resembling the phospholipid composition of the inner leaflet of the outer membrane of *Salmonella typhimurium* being composed of the same constituents as that of the other strains used [46]. For electrical measurements, planar membranes were voltage-clamped via a pair of Ag/AgCl electrodes (type IVM E-255, Science Products, Hofheim, Germany) connected to the headstage of an L/M-PCA patch-clamp amplifier (List-Medical, Darmstadt, Germany). In all experiments, the compartment to which peptide was added is named first, and the compartment opposite to the addition was grounded. In comparison to the natural system, a positive clamp voltage represents a membrane with negative potential on the inside. All measurements were performed at a temperature of 37°C in 5 mM HEPES, 100 mM KCl, 5 mM $MgCl_2$, pH 7.0. Two electrical parameters were determined: (i) current through

peptide-induced lesions and (ii) peptide-induced changes of the membrane capacitance. Assuming a plate condensator model, the membrane capacitance yields information about the area, thickness, and composition of the bilayer. Using small positive and negative jumps of the clamp voltage, the maximum voltage required to determine membrane capacitance is <1 mV. Therefore, peptide membrane interaction can be investigated without the influence of a significant external potential. This method allows the determination of changes in membrane capacitance with a precision of <1 pF.

RESULTS

Antibacterial activity of peptides

We tested the activity of NK-2, of the fluorescently labelled peptide NBD-NK-2, and of the shortened variant NK11 against two bacterial strains we have established in our lab as source for the extraction of highly purified and well characterized deep rough mutant LPS. These were *E. coli* WBB01 and *P. mirabilis* R45. The latter has been reported to be resistant to many cationic antimicrobial peptides and in particular to polymyxin B. The LPS structures of these strains differ by the degree of substitution with cationic aminoarabinose residues at the head group phosphates or at the first Kdo sugar. This results in variations in charge distribution and total net charges of –4 and –3 for *E. coli* WBB01 and *P. mirabilis* R45 LPS, respectively [35]. We also tested two internal reference strains from *S. enterica* with variations in the LPS structure: strain R60 with LPS Ra chemotype, i.e. complete core sugar, and the deep rough mutant strain R595 with LPS Re chemotype. The minimum peptide concentrations necessary to inhibit bacterial growth (MIC) and to kill bacteria (MBC) were determined under two different salt conditions (Tab. 1). The peptide NK-2 exhibited excellent activity against all used strains in low salt buffer. In physiological salt concentration, however, the activity against *P. mirabilis* was considerably impaired. The fluorescently labelled NBD-NK-2 exhibited almost the same activity as NK-2, i.e. the MIC/MBC values varied within one dilution step. The shortened version of NK-2, NK11 was almost inactive. The well known AMPs polymyxin B and melittin served as references. As demonstrated before, the activity of polymyxin B against *P. mirabilis* was extremely salt sensitive [41].
The differences in growth inhibiting and in bactericidal concentrations of NK-2 were also reflected in the killing kinetics. *E. coli* WBB01 was completely eradicated after 10 min of incubation with 5 µM NK-2, whereas the growth of *P. mirabilis* was reduced but not inhibited even after over night incubation by the same concentration of peptide (Fig. 1).

Influence of peptides on the ultrastructure of bacteria

The morphological changes of *E. coli* WBB01 and *P. mirabilis* R45 upon treatment with NK-2 and NK11 were visualized by TEM and AFM. NK-2 induced membrane blebbing, membrane ruffling, membrane detachment, and formation of electron dense dots in- and outside the cells of both strains (Fig. 2, 3). Furthermore, the surface roughness of bacteria increased in the presence of the peptide (Fig. 4 B, E). This effect was even more pronounced for *P. mirabilis*. Additionally, NK-2 evoked distinct processes in the cytoplasm of the bacteria. The peptide induced the release of cytoplasmic material from *E. coli* (Fig. 2) and the formation of electron dense fibrous structures in *P. mirabilis* (Fig. 3 G, I). In sharp contrast, no profound differences were evident between NK11-treated bacteria and controls (Fig. 2, 3). Only minor alterations of the bacterial surface were visible (Fig. 4). Peptide-induced changes of the bacterial morphology corresponded with viability. After incubation of bacteria with peptides, aliquots of the bacterial suspensions were plated out on LB agar plates and incubated over night. Colony growth of *E. coli* was completely inhibited by 2 µM NK-2, while 20 µM NK-2 reduced the growth of *P. mirabilis* colonies by 54%. NK11 (20 µM) had

no effect on the viability of both strains.

Binding of fluorescently labelled NK-2 to live bacteria

Peptide binding to live bacteria was analyzed by FACS by measuring the green fluorescence (FL1) of single bacteria after incubation with the fluorescently labelled peptide NBD-NK-2 (Fig. 5). Dotplots of the FSC signal against the green fluorescent signal (FL1-Area) for *E. coli* WBB01 without and with NBD-labelled NK-2 are shown in Fig. 5 A and B, respectively. The fluorescence intensity of NBD-NK-2 bound to bacteria was measured and normalized to that of *E. coli*. This relative fluorescence signal (FL-1 Area) was 1.0 for *E. coli* WBB01 and 0.36±0.14 for *P. mirabilis* R45, respectively (Fig. 5C). Thus the binding of NBD-NK-2 to *P. mirabilis* was strongly impaired compared to *E. coli*.

Permeabilization of bacterial membranes

As the observed ultrastructure of NK-2-treated bacteria strongly suggested a membranolytic step in the mode of action of this peptide, we investigated the uptake of a DNA-intercalating dye, SYTOX green, by a suitable bacterial strain, i.e. *E. coli* WBB01, during incubation with NK-2, NK11 and melittin. Dye uptake directly reflects membrane permeabilization, as SYTOX green itself cannot permeate through an intact lipid bilayer. In the case of Gram-negative bacteria, inner and outer membrane permeabilization is apparently necessary to accomplish dye uptake. A dose-dependent uptake of the fluorescent dye was observed for bacteria treated with NK-2 and melittin (Fig. 6). In contrast, no increase of fluorescence was induced by NK11. The peptide concentration necessary to induce dye uptake in *E. coli* WBB01 correlated with the MIC of NK-2, however, occurred at a concentration considerably below the MIC for melittin.

Secondary structure of peptides

The secondary structures of NK-2, and NK11 were analyzed by CD spectroscopy. Both peptides appeared without defined structure in buffer [26]. When added to an aggregate suspension of *E. coli* WBB01 LPS, however, NK-2 adopted an ordered structure with a pronounced higher α–helical content than NK11 (Fig. 7). Apparently, the spectrum of NK-2 in the presence of LPS does not reflect all characteristics of a typical CD spectrum of an α-helical peptide [47], which has been observed earlier for NK-2 in the presence of TFE and SDS [11, 26, 27]. Whereas the bands at 190 nm and 222 nm are visible in the CD spectrum of NK-2 in the presence of LPS, the negative band at 208 nm is drastically reduced due to the interference with LPS and light scattering effects due to LPS aggregates. LPS alone produces already a strong CD signal, so that the interaction between polarized light and LPS interferes with its peptide interaction. Light scattering due to LPS particles is another problem which disturbs the CD spectrum. However, a deconvolution of the CD spectrum into contributions of different secondary structure elements using CONTIN/LL shows that the α-helix content is around 50 %. The CD spectrum of NK11 is very low in intensity and difficult to analyze in terms of secondary structure elements. The α-helix content is clearly much lower compared with NK-2, and there are strong contributions from unordered peptides.

Binding of peptides to solid-supported LPS bilayers

Binding of NK-2 and NK11 to LPS bilayers was monitored in real time using the SAW biosensor. Injection of suspensions of *E. coli* WBB01 LPS and of *P. mirabilis* R45 LPS led to the formation of LPS bilayers on top of a PLL layer (not shown), and induced a phase shift of 82±18 ° and of 162±23 °, respectively. Phase shifts induced by subsequent peptide injections were normalized to the LPS-induced phase shift, i.e. to the mass loading of the LPS bilayer (Fig. 8). Both peptides induced a phase shift after injection (each 100 µM) to LPS bilayers constituted of *E. coli* LPS WBB01, or of *P. mirabilis* LPS R45, indicating peptide-

LPS binding in all cases. The maximal normalized increase of the phase induced by NK-2 injection was 84% and 44% for bilayers of *E. coli* LPS WBB01, and of *P. mirabilis* LPS R45, respectively. By NK11 injection the corresponding values were 14% and 18%. Therefore, the amount of NK-2 bound to the bilayer of *E. coli* LPS was twice as much as the amount of peptide bound to the bilayer of *P. mirabilis* LPS under the same conditions. Off rates were low for NK-2 but high for NK11, demonstrating significant differences in LPS binding affinities of the two peptides. To address salt dependency of the peptide-LPS interaction, we compared the binding of NK-2 to LPS in 20 mM HEPES, pH 7.0 and in the same buffer with additional 150 mM NaCl. The observed binding curves were very similar (not shown), suggesting that the ionic strength has no major impact on the amount of peptide bound to the LPS bilayer.

Insertion of peptides into the bilayer of LPS aggregates

FRET spectroscopy served as a sensitive tool for the insertion kinetics of NK-2 and NK11 into LPS bilayers. The peptides were added to LPS aggregates doped with the FRET pair NBD- and rhodamine-PE. A strong, dose-dependent increase of the FRET-signal was observed immediately after NK-2 addition indicating a fast insertion into the LPS aggregate. Eventually, the FRET signal reached a plateau value, similar for the two LPS (Fig. 9A, B). In contrast, addition of NK11 led to a reduced FRET signal, i.e. enhanced FRET efficacy, indicating a different mode of interaction. We suggest that NK11 did not intercalate into the lipid aggregate but bound superficially and induced the segregation of LPS and of PE. Hence, labelled PE were accumulated, which account for an increased FRET probability. Notably, differences in the ionic strength of the buffer have only a negligible influence on intercalation of the peptides into bilayers of LPS of *P. mirabilis* R45 (Fig. 9B, C) and of LPS of *E. coli* WBB01 (not shown).

Lesion formation by NK-2 in symmetric phospholipid and in asymmetric LPS/phospholipid planar lipid bilayers

The formation of membrane lesions or pores by the peptide NK-2 was done by the Montal-Mueller planar lipid bilayer technique. This system allows the reconstitution of membranes with virtually any lipid composition, including a symmetrical membrane of a defined phospholipid mixture (PL) mimicking roughly the cytoplasmic membrane of bacteria. Furthermore, it allows mimicking the asymmetrical outer membrane of Gram-negative bacteria consisting of LPS on its outer leaflet and of PL on its inner leaflet (LPS/PL). We determined the membrane capacitance as a measure of peptide/membrane interaction and measured the emerging current fluctuations while a transmembrane potential was applied. The peptide was always added to one side of the membrane, in case of the asymmetric LPS/PL membrane to the LPS side. After addition of NK-2 to a symmetric PL/PL or an asymmetric LPS/PL membrane, we observed initially a slight increase of membrane capacitance followed by a significant decrease of about 5-20% before the formation of any lesions or pores. A representative curve for a symmetric PL/PL membrane is depicted in Fig. 10. Since membrane capacitance is a result of many different factors (i.e. membrane thickness, area, and dielectricity) we cannot assign the factor or factors which are influenced by the peptide, however, the change of capacitance is a clear-cut indicator that an interaction takes place. After applying a transmembrane potential (negative inside), single current fluctuations were observed at -20 mV, which in the case of the symmetric PL/PL bilayer accumulate already at this low voltage over time. Finally, this led to the disruption of the membrane (Fig. 10). No current fluctuations were observed for NK11 under the same conditions (not shown). After the addition of NK-2 to asymmetric LPS/PL bilayers, we obtained current fluctuations of 50 pA to more than 400 pA at -100 mV (Fig. 11). These lesions were unstructured and heterogeneous without a clear gating characteristic and the induction of lesions seemed to be

cooperative. Eventually, the number and/or size of lesions increased dramatically and the integrity of the membrane was destroyed (not shown). In some cases, however, we observed a stable integration of the peptide NK-2 into the membrane resulting in defined conductance levels and gating (Fig. 12). They exhibited conductance levels up to 24 nS, which were relatively independent of the voltage polarity. No pronounced differences of the NK-2-induced lesions between the two types of LPS membranes were observed.

It should be emphasized that each planar lipid bilayer experiment is unique and we selected representative current traces for figures 10-12. However, due to the experimental setup, we cannot rule out stochastic events, which are apparently the reason for the formation of lesions with a defined conductance level (Fig. 12). Asymmetric bilayers (LPS/PL) with one monolayer of the membrane composed of LPS and the other one composed of a phospholipid (PL) mixture behave differently than symmetric PL/PL bilayers. Whereas PL/PL bilayers were immediately destabilized after the addition of NK-2 (Fig. 10), LPS/PL bilayers were of higher stability. In most experiments with asymmetric membranes, we observed heterogeneous lesions (Fig. 11), which were indistinguishable from those lesions observed in PL/PL bilayers. However, contrary to PL/PL bilayers, NK-2-induced lesions in LPS/PL bilayers sometimes closed spontaneously. This inherent membrane stability may be the reason for the stochastic formation of lesions with a defined conductance level (Fig. 12).

DISCUSSION

The NK-lysin derived peptide NK-2 exhibits activity against a wide range of Gram-negative bacteria, whereas its shortened derivative NK11 is almost inactive [26, 31]. In this study, we asked three major questions: 1) Is NK-2-induced killing of Gram-negative bacteria mediated by membrane permeabilization, and what are the characteristics of NK-2-induced membrane lesions? Which types of model membranes are suitable 2) to allow a discrimination between a peptide with potent activity against Gram-negative bacteria and an inactive peptide, and 3) to explain the differential activity of a certain peptide against two Gram-negative bacterial strains? These questions have been investigated representatively with NK-2 and NK11 against *E. coli* WBB01 and *P. mirabilis* R45.

In several previous investigations, we have documented the surface activity of NK-2 [27] and its impact on artificial membranes composed of phospholipids [25, 26, 33] and LPS [31]. However, the direct link between artificial membranes and intact bacterial membranes is still missing. Here, we provide convincing evidences that a direct peptide-membrane interaction is involved in antibacterial action of NK-2: i) The killing of *E. coli* was rapid, also the delayed killing of *P. mirabilis* cultures does not necessarily exclude rapid killing of a single bacteria, and ii) was accompanied by dramatic changes of the bacterial morphology. The surface roughness increased upon peptide interaction and membrane effects such as membrane ruffling and detachment of the outer and inner membrane took place. Morphological membrane damage and membrane detachment have also been shown for other peptides and appear to be general features of membranolytic peptides such as melittin, lactoferricin B, and hecate 1 [48-50]. The observed changes distinguish lytic peptides from those membrane-interacting peptides acting primarily by a non-lytic mechansim such as human psoriasin [51]. iii) Even more convincing, NK-2 (and also melittin) permeabilized the membranes of viable *E. coli* cells as evidenced by uptake of the fluorescent DNA-intercalating dye SYTOX green by the bacteria. iv) NK-2 concentrations necessary to induce bacterial killing, to permeabilize bacterial membranes, as well as to induce measurable effects on the artificial LPS model membranes were very similar. All findings together strongly support the thesis that LPS interaction and outer membrane permeabilization are crucial for bacterial killing by NK-2.

Recently, we have analyzed the activity of NK-2–derived peptides against Gram-negative bacterial strains [26]. However, the applied simple artificial membrane system (PG liposomes), which was formerly sufficient to explain the target cell selectivity of NK-2 [25], failed to explain different activities of the tested peptides. In particular, PG was not a suitable model to explain differences in activity between the parent peptide NK-2 and NK11. The inactivity of NK11 was not due to its inability to interact with negatively charged lipid membranes in general. As we have shown earlier, NK11, like NK-2, intercalated into PG membranes [26]. Here, we show that peptide interactions with the bacterial outer membrane lipids, i.e. LPS, determine whether bacteria are killed or not. This is demonstrated by significant differences in amounts and affinities of NK-2 vs NK11 binding to solid supported LPS bilayers on a polymer cushion. Moreover, NK-2 desorption from the LPS bilayer was very slow indicating a high binding affinity. Upon contact with LPS containing membranes, the peptide NK-2, but not NK11, adopted a defined, mostly α–helical, secondary structure. NK-2 intercalated into all tested LPS bilayer membranes, as demonstrated by FRET spectroscopy, whereas no intercalation was observed for NK11. Eventually, NK-2 induced transient, heterogeneous lesions without a clear gating characteristic in symmetric and asymmetric planar lipid bilayers mimicking the cytoplasmic and the outer membranes of *E. coli* and *P. mirabilis*. Stable integration of NK-2 was observed into asymmetric LPS/PL bilayers, but not in symmetric PL/PL bilayers, underlining the importance of the choice of lipids for peptide/membrane-interaction studies. The conductivity of these stable lesions was independent of the applied voltage polarity, which suggests a symmetrical pore structure. This is in contrast to the conductivity of membrane lesions induced by human β-defensin 3 in LPS/PL bilayers, which was strongly dependent on the voltage polarity and which indicated an asymmetry in pore geometry or charge distribution [38].

The concentration of NK-2 necessary to kill *P. mirabilis* was higher than that to kill *E. coli*. This tendency was even more distinctive when NaCl was added at physiological concentration, suggesting that electrostatic interactions may be important for the antibacterial activity of NK-2. Moreover, this phenomenon was also observed with two reference AMPs used in this study, namely melittin and polymyxin B. The latter, which was completely inactive against *P. mirabilis* at physiological salt concentration rendered highly active in low ionic strength buffer. The used LPS from *E. coli* and *P. mirabilis* differ in the number of core carbohydrates and phosphate groups attached to aminoarabinose residues. These changes result in an altered charge distribution and slightly reduced net charge for *P. mirabilis* LPS [35, 38]. Consistently, the enthalpy change of the binding reaction of NK-2 to LPS of *P. mirabilis* was lowered in the presence of 150 mM NaCl compared to buffer without salt (not shown). This is an apparent contradiction to the biosensor and FRET measurements which suggest that the binding and insertion of NK-2 into LPS is independent on the ionic strength. Currently, we have no satisfactorily explanation for this behaviour and we will investigate this issue in future studies. Besides electrostatic attraction, also other factors such as osmotic stress have to be considered to explain the salt-dependence of the antibacterial activity of NK-2 and other peptides. In Gram-negative bacteria, osmotic effects should be restricted to the cytoplasmic membrane. The presence of porins in the outer membrane enable the free flux of ions and thus prevent the emergence of osmotic pressure.

Interestingly, neither intercalation of NK-2 nor permeabilization of model membranes by this peptide appeared to be dependent on the differing LPS carbohydrate structures of the two tested LPS. Hence, these processes do not contribute to differences in biological activity. From the analysis of the interaction of fluorescently labeled NK-2 with viable bacteria and from biosensor data it is apparent that improved LPS binding of NK-2 is important for an enhanced activity against *E. coli* WBB01 compared to *P. mirabilis*. Thus, it may be concluded that electrostatic attraction of the peptide to the bacterial surface is the decisive step in the killing process, and that intercalation of NK-2 into the hydrophobic acyl chain region of the

membrane and subsequent permeabilization of the bacterial membranes are independent of the chemical structure of the LPS sugar part. A similar molecular basis for target discrimination has been described for protegrin action on *Pseudomanas aeruginosa* and *Burkholderia cepacia* [52]. Also different principles are known for other AMPs such as human β-defensin 3, and polymyxin B, where the emergence and the size of LPS membrane lesions have been made responsible for activity, respectively [35, 38].

Besides membranes also intracellular structures have been discussed as targets for AMPs [9, 53]. For several peptides, a cytoplasmic localization has been demonstrated [54, 55] or ruled out [56]. Membrane permeabilization and disturbance are important first steps in bacterial killing by NK-2, it should be mentioned, however, that this peptide also elicits bacteria-specific effects inside the cytoplasm, such as cytoplasmic retraction and formation of filamentous structures, suggesting that secondary targets of NK-2 are intracellular structures, such as DNA, or that the impact of NK-2 on the bacterial membrane results in clustering or rearrangement of these intracellular structures.

In summary, NK-2 binds to the surface of Gram-negative bacteria and also to LPS model membranes and subsequently permeabilizes bacterial membranes as well as artificial lipid bilayers composed of LPS. LPS binding affinity clearly differentiates active NK-2 from inactive NK11. We conclude that the LPS carbohydrate structures determine the binding affinity of the peptides to the bacterial surface and thus their biological activities. Our data stress the importance of membrane reconstitution systems which closely resemble the lipid compositions of their natural counterparts.

Acknowledgements

We thank Rainer Bartels for peptide synthesis, Jan Demmer for AFM measurements, Christine Hamann for FRET spectroscopy, Heike Kühl for electron microscopy, and Kerstin Stephan for performing the antibacterial tests.

Funding

This study has been carried out with financial support from the Deutsche Forschungsgemeinschaft (SFB 617 ´Molecular mechanisms of epithelial defense´, project A17).

REFERENCES

1 Levy, S. B. and Marshall, B. (2004) Antibacterial resistance worldwide: causes, challenges and responses. Nat. Med. **10**, S122-129

2 Norrby, S. R., Nord, C. E. and Finch, R. (2005) Lack of development of new antimicrobial drugs: a potential serious threat to public health. Lancet Infect. Dis. **5**, 115-119

3 Zasloff, M. (2002) Antimicrobial peptides of multicellular organisms. Nature. **415**, 389-395

4 Hancock, R. E. and Sahl, H. G. (2006) Antimicrobial and host-defense peptides as new anti-infective therapeutic strategies. Nat. Biotechnol. **24**, 1551-1557

5 Overhage, J., Campisano, A., Bains, M., Torfs, E. C., Rehm, B. H. and Hancock, R. E. (2008) Human host defense peptide LL-37 prevents bacterial biofilm formation. Infect. Immun. **76**, 4176-4182

6 Shai, Y. (2002) Mode of action of membrane active antimicrobial peptides. Biopolymers. **66**, 236-248

7 Hancock, R. E. and Rozek, A. (2002) Role of membranes in the activities of antimicrobial cationic peptides. FEMS Microbiol. Lett. **206**, 143-149
8 Bechinger, B. and Lohner, K. (2006) Detergent-like actions of linear amphipathic cationic antimicrobial peptides. Biochim. Biophys. Acta. **1758**, 1529-1539
9 Brogden, K. A. (2005) Antimicrobial peptides: pore-formers or metabolic inhibitors in bacteria. Nat. Rev. Microbiol. **3**, 238-250
10 Hale, J. D. and Hancock, R. E. (2007) Alternative mechanisms of action of cationic antimicrobial peptides on bacteria. Expert Rev. Anti Infect. Ther. **5**, 951-959
11 Andrä, J. and Leippe, M. (1999) Candidacidal activity of shortened synthetic analogs of amoebapores and NK-lysin. Med. Microbiol. Immunol. **188**, 117-124
12 Andersson, M., Gunne, H., Agerberth, B., Boman, A., Bergman, T., Sillard, R., Jörnvall, H., Mutt, V., Olsson, B., Wigzell, H., Dagerlind, A., Boman, H. G. and Gudmundsson, G. H. (1995) NK-lysin, a novel effector peptide of cytotoxic T and NK cells. Structure and cDNA cloning of the porcine form, induction by interleukin 2, antibacterial and antitumour activity. EMBO J. **14**, 1615-1625
13 Peña, S. V., Hanson, D. A., Carr, B. A., Goralski, T. J. and Krensky, A. M. (1997) Processing, subcellular localization, and function of 519 (Granulysin), a human late T cell activation molecule with homology to small, lytic, granule proteins. J. Immunol. **158**, 2680-2688
14 Leippe, M., Andrä, J., Nickel, R., Tannich, E. and Müller-Eberhard, H. J. (1994) Amoebapores, a family of membranolytic peptides from cytoplasmic granules of *Entamoeba histolytica*: isolation, primary structure, and pore formation in bacterial cytoplasmic membranes. Mol. Microbiol. **14**, 895-904
15 Davis, E. G., Sang, Y., Rush, B., Zhang, G. and Blecha, F. (2005) Molecular cloning and characterization of equine NK-lysin. Vet. Immunol. Immunopathol. **105**, 163-169
16 Endsley, J. J., Furrer, J. L., Endsley, M. A., McIntosh, M. A., Maue, A. C., Waters, W. R., Lee, D. R. and Estes, D. M. (2004) Characterization of bovine homologues of granulysin and NK-lysin. J. Immunol. **173**, 2607-2614
17 Herbst, R., Ott, C., Jacobs, T., Marti, T., Marciano-Cabral, F. and Leippe, M. (2002) Pore-forming polypeptides of the pathogenic protozoon *Naegleria fowleri*. J. Biol. Chem. **277**, 22353-22360.
18 Vaccaro, A. M., Salvioli, R., Tatti, M. and Ciaffoni, F. (1999) Saposins and their interaction with lipids. Neurochem. Res. **24**, 307-314
19 Munford, R. S., Sheppard, P. O. and O'Hara, P. J. (1995) Saposin-like proteins (SAPLIP) carry out diverse functions on a common backbone structure. J. Lipid Res. **36**, 1653-1663
20 Liepinsh, E., Andersson, M., Ruysschaert, J.-M. and Otting, G. (1997) Saposin fold revealed by the NMR structure of NK-lysin. Nat. Struct. Biol. **4**, 793-795
21 Hecht, O., Van Nuland, N. A., Schleinkofer, K., Dingley, A. J., Bruhn, H., Leippe, M. and Grötzinger, J. (2004) Solution structure of the pore forming protein of *Entamoeba histolytica*. J. Biol. Chem. **279**, 17834-17841
22 Leippe, M., Andrä, J. and Müller-Eberhard, H. J. (1994) Cytolytic and antibacterial activity of synthetic peptides derived from amoebapore, the pore-forming peptide of *Entamoeba histolytica*. Proc. Natl. Acad. Sci. USA. **91**, 2602-2606
23 Andrä, J., Berninghausen, O., Wülfken, J. and Leippe, M. (1996) Shortened amoebapore analogs with enhanced antibacterial and cytolytic activity. FEBS Lett. **385**, 96-100
24 Leippe, M. (1995) Ancient weapons: NK-lysin is a mammalian homolog to pore-forming peptides of a protozoan parasite. Cell. **83**, 17-18
25 Schröder-Borm, H., Willumeit, R., Brandenburg, K. and Andrä, J. (2003) Molecular basis for membrane selectivity of NK-2, a potent peptide antibiotic derived from NK-

lysin. Biochim. Biophys. Acta. **1612**, 164-171

26 Andrä, J., Monreal, D., Martinez de Tejada, G., Olak, C., Brezesinski, G., Sanchez Gomez, S., Goldmann, T., Bartels, R., Brandenburg, K. and Moriyon, I. (2007) Rationale for the design of shortened derivatives of the NK-lysin derived antimicrobial peptide NK-2 with improved activity against Gram-negative pathogens. J. Biol. Chem. **282**, 14719-14728

27 Olak, C., Muenter, A., Andrä, J. and Brezesinski, G. (2008) Interfacial properties and structural analysis of the antimicrobial peptide NK-2. J. Pept. Sci. **14**, 510-517

28 Jacobs, T., Bruhn, H., Gaworski, I., Fleischer, B. and Leippe, M. (2003) NK-lysin and its shortened analog NK-2 exhibit potent activities against *Trypanosoma cruzi*. Antimicrob. Agents Chemother. **47**, 607-613

29 Gelhaus, C., Jacobs, T., Andrä, J. and Leippe, M. (2008) The antimicrobial NK-2 peptide, the core region of mammalian NK-lysin, kills intraerythrocytic *Plasmodium falciparum*. Antimicrob. Agents Chemother. **52**, 1713-1720

30 Schröder-Borm, H., Bakalova, R. and Andrä, J. (2005) The NK-lysin derived peptide NK-2 preferentially kills cancer cells with increased surface levels of negatively charged phosphatidylserine. FEBS Lett. **579**, 6128-6134

31 Andrä, J., Koch, M. H. J., Bartels, R. and Brandenburg, K. (2004) Biophysical characterization of the endotoxin inactivation by NK-2, an antimicrobial peptide derived from mammalian NK-Lysin. Antimicrob. Agents Chemother. **48**, 1593-1599

32 Lohner, K. and Prenner, E. J. (1999) Differential scanning calorimetry and X-ray diffraction studies of the specificity of the interaction of antimicrobial peptides with membrane-mimetic systems. Biochim. Biophys. Acta. **1462**, 141-156

33 Willumeit, R., Kumpugdee, M., Funari, S. S., Lohner, K., Pozo Navas, B., Brandenburg, K., Linser, S. and Andrä, J. (2005) Structural rearrangement of model membranes by the peptide antibiotic NK-2. Biochim. Biophys. Acta. **1669**, 125-134

34 Hancock, R. E. W. (1997) Peptide antibiotics. Lancet. **349**, 418-422

35 Wiese, A., Münstermann, M., Gutsmann, T., Lindner, B., Kawahara, K., Zähringer, U. and Seydel, U. (1998) Molecular mechanisms of polymyxin B-membrane interactions: direct correlation between surface charge density and self-promoted transport. J. Membr. Biol. **162**, 127-138

36 Andrä, J., Lohner, K., Blondelle, S. E., Jerala, R., Moriyón, I., Koch, M. H. J., Garidel, P. and Brandenburg, K. (2005) Enhancement of endotoxin neutralization by coupling of a C12-alkyl chain to a lactoferricin-derived peptide. Biochem. J. **385**, 135-143

37 Gutsmann, T., Hagge, S. O., David, A., Roes, S., Böhling, A., Hammer, M. U. and Seydel, U. (2005) Lipid-mediated resistance of Gram-negative bacteria against various pore-forming antimicrobial peptides. J. Endotoxin Res. **11**, 167-173

38 Böhling, A., Hagge, S. O., Roes, S., Podschun, R., Sahly, H., Harder, J., Schröder, J. M., Grötzinger, J., Seydel, U. and Gutsmann, T. (2006) Lipid-specific membrane activity of human beta-defensin-3. Biochemistry. **45**, 5663-5670

39 Galanos, C., Lüderitz, O. and Westphal, O. (1969) A new method for the extraction of R lipopolysaccharides. Eur. J. Biochem. **9**, 245-249

40 Andrä, J., Hammer, M. U., Grötzinger, J., Jakovkin, I., Lindner, B., Vollmer, E., Fedders, H., Leippe, M. and Gutsmann, T. (2009) Significance of the cyclic structure and of arginine residues for the antibacterial activity of arenicin-1 and its interaction with phospholipid and lipopolysaccharide model membranes. Biol. Chem. **390**, 337-349

41 Andrä, J., Jakovkin, I., Grötzinger, J., Hecht, O., Krasnosdembskaya, A. D., Goldmann, T., Gutsmann, T. and Leippe, M. (2008) Structure and mode of action of the antimicrobial peptide arenicin. Biochem. J. **410**, 113-122

42 Andrä, J., Böhling, A., Gronewold, T. M. A., Schlecht, U., Perpeet, M. and Gutsmann,

T. (2008) Surface acoustic wave biosensor as a tool to study the interaction of antimicrobial peptides with phospholipid and lipopolysaccharide model membranes. Langmuir. **24**, 9148-9153

43 Schromm, A. B., Brandenburg, K., Rietschel, E. T., Flad, H. D., Carroll, S. F. and Seydel, U. (1996) Lipopolysaccharide-binding protein mediates CD14-independent intercalation of lipopolysaccharide into phospholipid membranes. FEBS Lett. **399**, 267-271

44 Montal, M. and Mueller, P. (1972) Formation of bimolecular membranes from lipid monolayers and a study of their electrical properties. Proc. Natl. Acad. Sci. USA. **69**, 3561-3566

45 Wiese, A. and Seydel, U. (2000) Electrophysiological measurements on reconstituted outer membranes. Methods Mol. Biol. **145**, 355-370

46 Shaw, N. (1974) Lipid composition as a guide to the classification of bacteria. Adv. Appl. Microbiol. **17**, 63-108

47 Fasman, G. D. (1996) Circular dichroism and the conformational analysis of biomolecules. Plenum Press, New York

48 Velasco, J., Bengoechea, J. A., Brandenburg, K., Lindner, B., Seydel, U., Gonzalez, D., Zähringer, U., Moreno, E. and Moriyón, I. (2000) Brucella abortus and its closest phylogenetic relative, Ochrobactrum spp., differ in outer membrane permeability and cationic peptide resistance. Infect. Immun. **68**, 3210-3218

49 van der Kraan, M. I., van Marle, J., Nazmi, K., Groenink, J., van 't Hof, W., Veerman, E. C., Bolscher, J. G. and Nieuw Amerongen, A. V. (2005) Ultrastructural effects of antimicrobial peptides from bovine lactoferrin on the membranes of *Candida albicans* and *Escherichia coli*. Peptides. **26**, 1537-1542

50 Henk, W. G., Todd, W. J., Enright, F. M. and Mitchell, P. S. (1995) The morphological effects of two antimicrobial peptides, hecate-1 and melittin, on *Escherichia coli*. Scanning Microsc. **9**, 501-507

51 Gläser, R., Harder, J., Lange, H., Bartels, J., Christophers, E. and Schröder, J. M. (2005) Antimicrobial psoriasin (S100A7) protects human skin from *Escherichia coli* infection. Nat. Immunol. **6**, 57-64

52 Albrecht, M. T., Wang, W., Shamova, O., Lehrer, R. I. and Schiller, N. L. (2002) Binding of protegrin-1 to *Pseudomonas aeruginosa* and *Burkholderia cepacia*. Respir. Res. **3**, 18

53 Wu, M., Maier, E., Benz, R. and Hancock, R. E. (1999) Mechanism of interaction of different classes of cationic antimicrobial peptides with planar bilayers and with the cytoplasmic membrane of *Escherichia coli*. Biochemistry. **38**, 7235-7242

54 Haukland, H. H., Ulvatne, H., Sandvik, K. and Vorland, L. H. (2001) The antimicrobial peptides lactoferricin B and magainin 2 cross over the bacterial cytoplasmic membrane and reside in the cytoplasm. FEBS Lett. **508**, 389-393

55 Powers, J. P., Martin, M. M., Goosney, D. L. and Hancock, R. E. (2006) The antimicrobial peptide polyphemusin localizes to the cytoplasm of *Escherichia coli* following treatment. Antimicrob. Agents Chemother. **50**, 1522-1524

56 Leptihn, S., Har, J. Y., Chen, J., Ho, B., Wohland, T. and Ding, J. L. (2009) Single molecule resolution of the antimicrobial action of quantum dot-labeled sushi peptide on live bacteria. BMC Biology. **7**, 22

FIGURE LEGENDS

Fig. 1. Time course of bacterial killing by NK-2. Bacteria ((A) *E. coli* WBB01, and (B) *P. mirabilis* R45) were incubated alone (control) and in the presence of 1 µM (open circles), 2 µM (filled circles), and 10 µM (open triangles) peptide in buffer (20 mM HEPES, 150 mM NaCl, pH 7.0) at 37°C. Viability of bacteria was assessed by plating out the bacterial suspensions at various time points and is presented as CFU (% of control) = ($CFU_{peptide}$ / $CFU_{control}$) * 100.

Fig. 2. Effect of peptide treatment on the morphology of bacteria (I). TEM images of *E. coli* WBB01. Bacteria were incubated alone (A, B), with 20 µM NK11 (D, E), and with 2 µM NK-2 (C, F-I). Length scale: each bar represents 1 µm. Arrows: (1) membrane blebs; (2) membrane ruffling; (3) membrane detachment; (4) electron dense dots; (5) release of cytoplasm; (6) electron dense fibres.

Fig. 3. Effect of peptide treatment on the morphology of bacteria (II). TEM images of *P. mirabilis* R45. Bacteria were incubated alone (A, B), with NK11 (D, E) and NK-2 (C, F-I) (each 20 µM). Length scale: each bar represents 1 µm. *, (C) bar represents 0.2 µm. Arrows: please refer to figure 2.

Fig. 4. Effect of peptide treatment on the morphology of bacteria (III). AFM images of (A-C) *E. coli* WBB01, and (D-F) *P. mirabilis* R45. Bacteria were incubated alone (A, D), with NK-2 (B: 2 µM, E: 20 µM) and NK11 (20 µM, C and F). Images were taken in air in AC (tapping) mode. Length (bar) and height (colour code) scales are indicated.

Fig. 5. FACS analysis of the binding of NBD-NK-2 to bacterial strains *E. coli* WBB01 and *P. mirabilis* R45. Dotplots of forward scattered light (FSC) against area of relative intensity of green light (FL-1 Area) for (A) *E. coli* WBB01 and (B) *E. coli* WBB01 incubated with 10 µM NBD-NK-2. (C) The amount of NBD-NK-2 bound to both strains of bacteria is shown normalized to peptide bound to *E. coli* WBB01.

Fig. 6. Permeabilization of bacterial membranes by AMPs. Damage of both the outer and inner membrane of *E. coli* WBB01 induced by NK-2 (filled circles), NK11 (open circles), and melittin (open triangles). Peptides were incubated with bacteria for 30 min. Permeabilization was monitored via the uptake of the DNA-intercalating fluorescent dye SYTOX green.

Fig. 7. CD spectra of NK-2 (black line) and NK11 (grey line) in the presence of a suspension of *E. coli* WBB01 LPS aggregates.

Fig. 8. Binding curves of NK-2 (black lines) and NK11 (grey lines) to bilayers of LPS from (A) *E. coli* WBB01 and (B) *P. mirabilis* R45. Peptides injections (start and end points are indicated by arrows) last 10 min (adsorption) followed by 10 min buffer rinse (desorption).

Fig. 9. Dose-dependent interaction of NK-2 (solid lines: black, 0.8 µM; grey 0.4 µM, light grey 0.2 µM) and NK11 (3 µM, dotted black line) with LPS membranes. Peptide intercalation into aggregates of LPS from (A) *E. coli* WBB01, and (B) *P. mirabilis* R45 in 20 mM HEPES, 150 mM NaCl, pH 7.0, and (C) *P. mirabilis* R45 in 20 mM HEPES, pH 7.0 was measured by by FRET spectroscopy at 37°C. Peptides were added at 50 s. An increase of the FRET-signal ($I_{Donor}/I_{Acceptor}$) corresponds to a reduced FRET efficiency and indicates insertion of peptide into the membrane.

Fig. 10. Representation of a typical planar lipid bilayer experiment. NK-2 (0.5 μM) was added at time point 0 min to a symmetrical PL/PL membrane mimicking the bacterial cytoplasmic membrane. Time courses of applied voltages (lower panel), peptide-induced capacity changes (upper panel, dotted grey line), and current traces (upper panel, black line) are shown. An arrow indicates disruption of the membrane.

Fig. 11. Time courses of NK-2-induced (0.3 μM) current traces and applied voltages in asymmetric planar lipid bilayers mimicking the outer membrane of Gram-negative bacteria: (A) *E. coli* WBB01 LPS/PL, and (B) *P. mirabilis* R45 LPS/PL.

Fig. 12. Stable integration of the peptide NK-2 (1 μM) into an asymmetric *E. coli* WBB01 LPS/PL planar lipid bilayer. After setting a clamp voltage, defined conductivity levels were reached.

Table 1 - Antibacterial activity

Activity of peptides against Gram-negative LPS rough mutant bacterial strains. The minimal inhibitory concentrations (MIC) and the minimal bactericidal concentrations (MBC) are given as MIC (MBC) in µg/ml. The assay was performed in (1) 20 mM Hepes pH 7.0, or in (2) 20 mM Hepes, 150 mM NaCl pH 7.0, each supplemented with 10% LB medium.

Bacterial strain	Buffer	NK-2	NBD-NK-2	NK11	Polymyxin B	Melittin
E. coli WBB01	1	4 (8)	8 (16)	>128 (>128)	1 (1)	2 (4)
	2	8 (16)	8 (16)	>128 (>128)	2 (2)	8 (16)
P. mirabilis R45	1	8 (32)	8 (32)	128 (>256)	1 (8)	8 (32)
	2	64 (>128)	64 (>128)	>256 (>256)	>256 (>256)	64 (128)
S. enterica R595	1	2 (4)	4 (4)	64 (>128)	2 (4)	2 (4)
	2	8 (16)	8 (8)	>256 (>256)	8 (16)	8 (16)
S. enterica R60	1	8 (16)	8 (16)	>128 (>128)	2 (4)	8 (16)
	2	8 (16)	16 (16)	>256 (>256)	4 (4)	32 (64)

Biochemical Journal Immediate Publication. Published on 26 Feb 2010 as manuscript BJ20091607

Figure 1

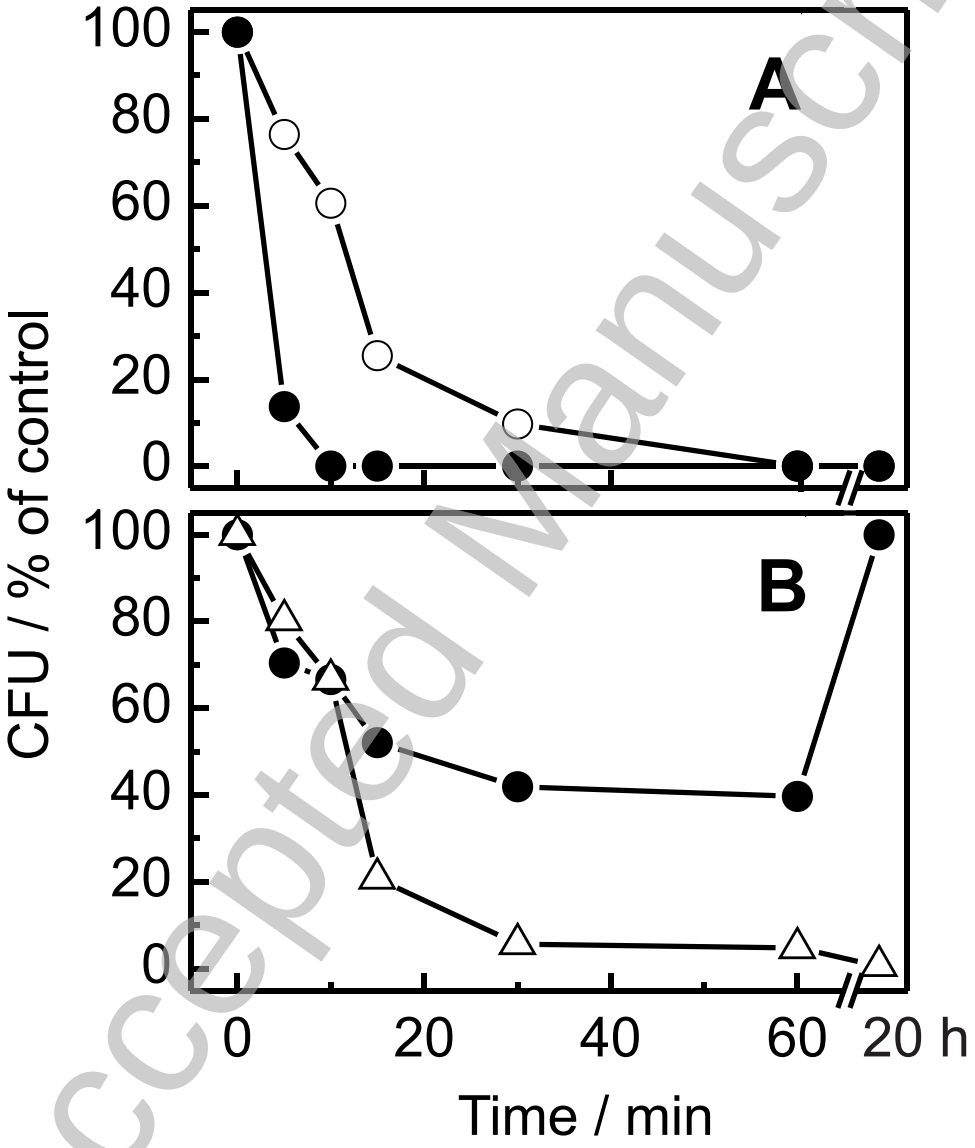

Biochemical Journal Immediate Publication. Published on 26 Feb 2010 as manuscript BJ20091607

Figure 2

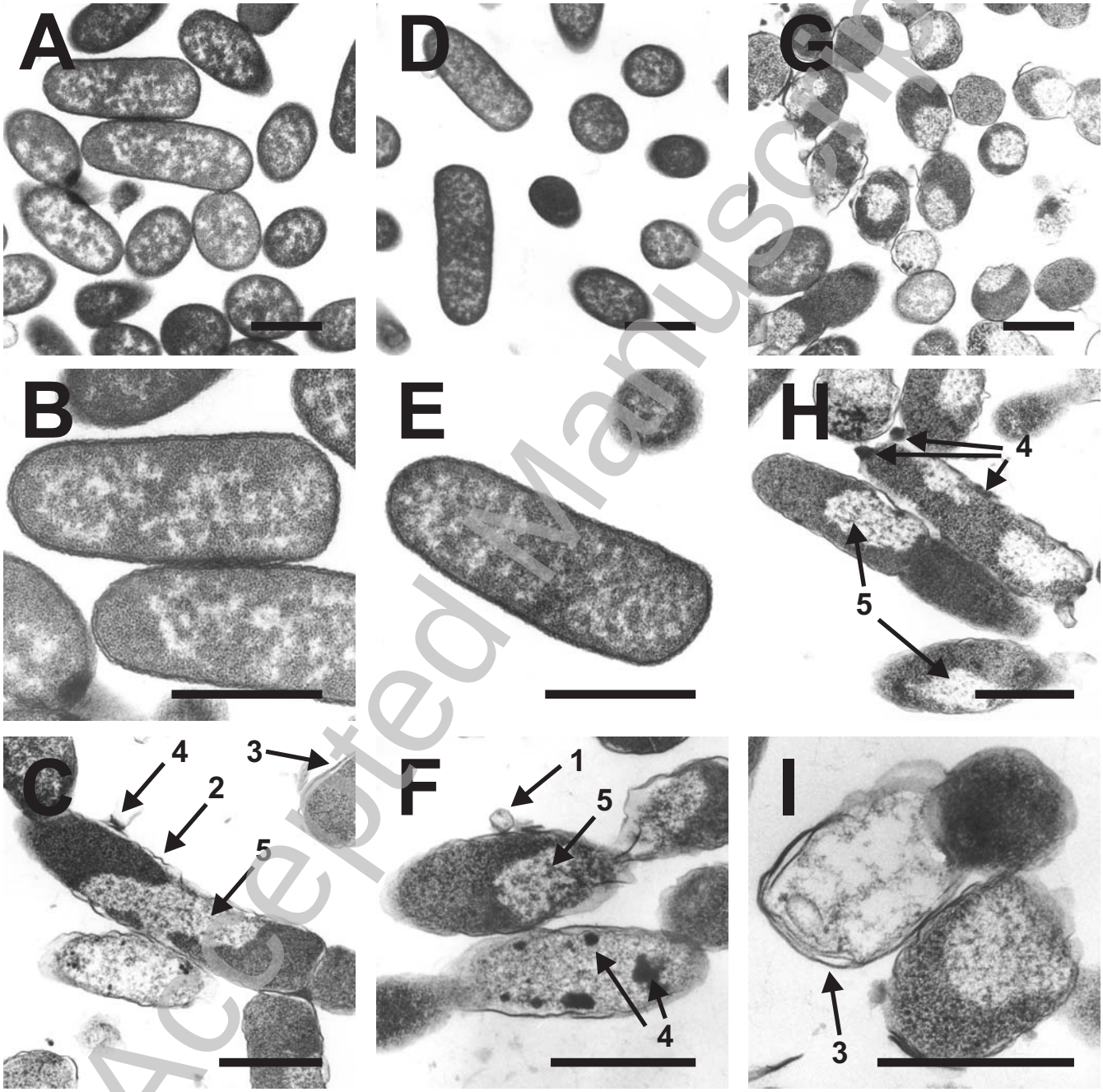

Biochemical Journal Immediate Publication. Published on 26 Feb 2010 as manuscript BJ20091607

Figure 3

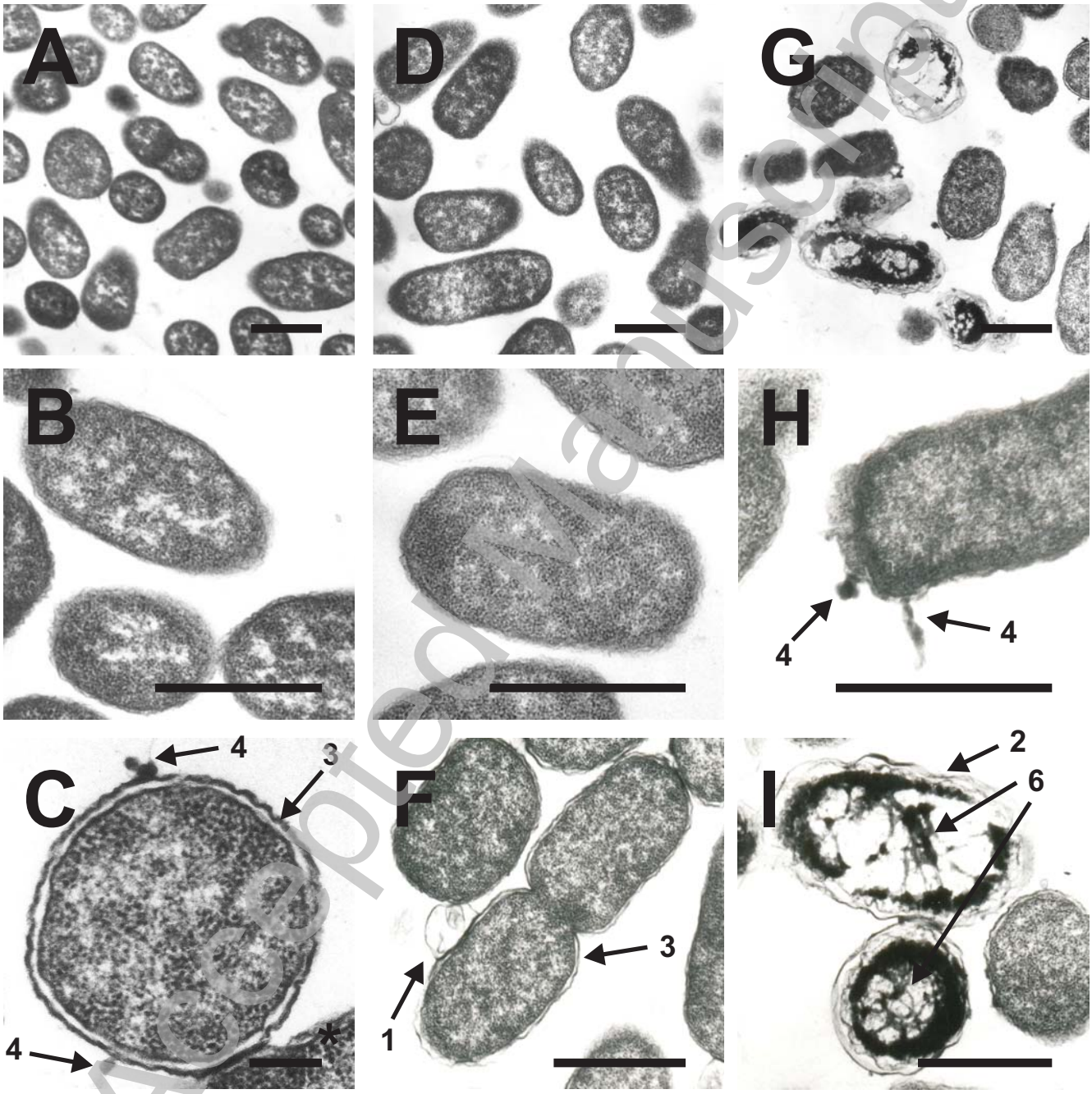

Biochemical Journal Immediate Publication. Published on 26 Feb 2010 as manuscript BJ20091607

Figure 4

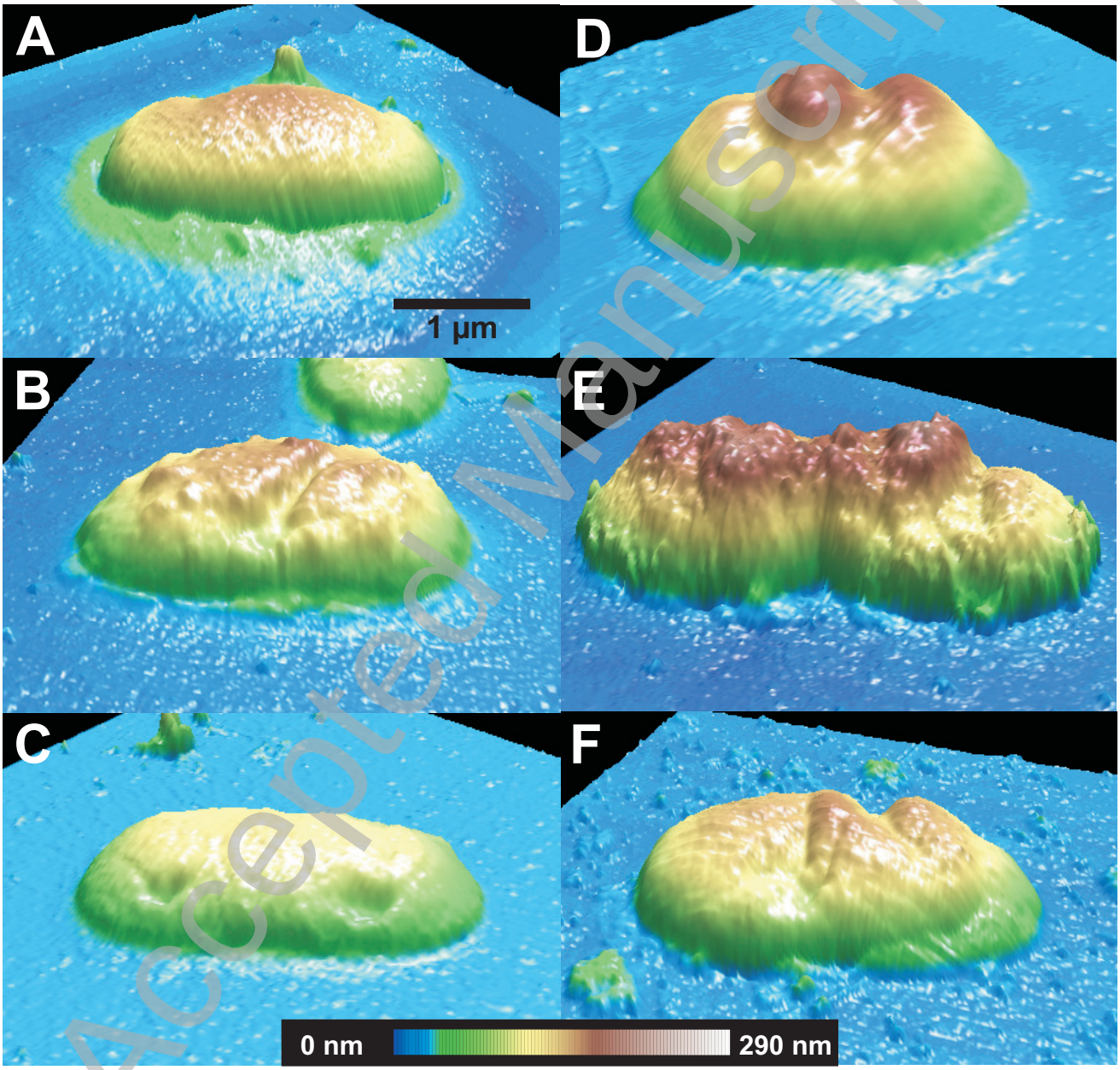

Biochemical Journal Immediate Publication. Published on 26 Feb 2010 as manuscript BJ20091607

Figure 5

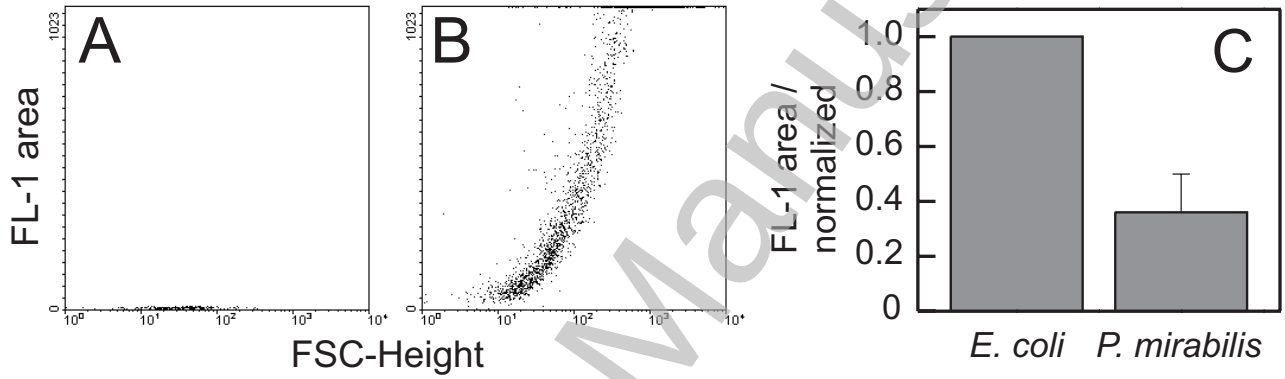

Biochemical Journal Immediate Publication. Published on 26 Feb 2010 as manuscript BJ20091607

Figure 6

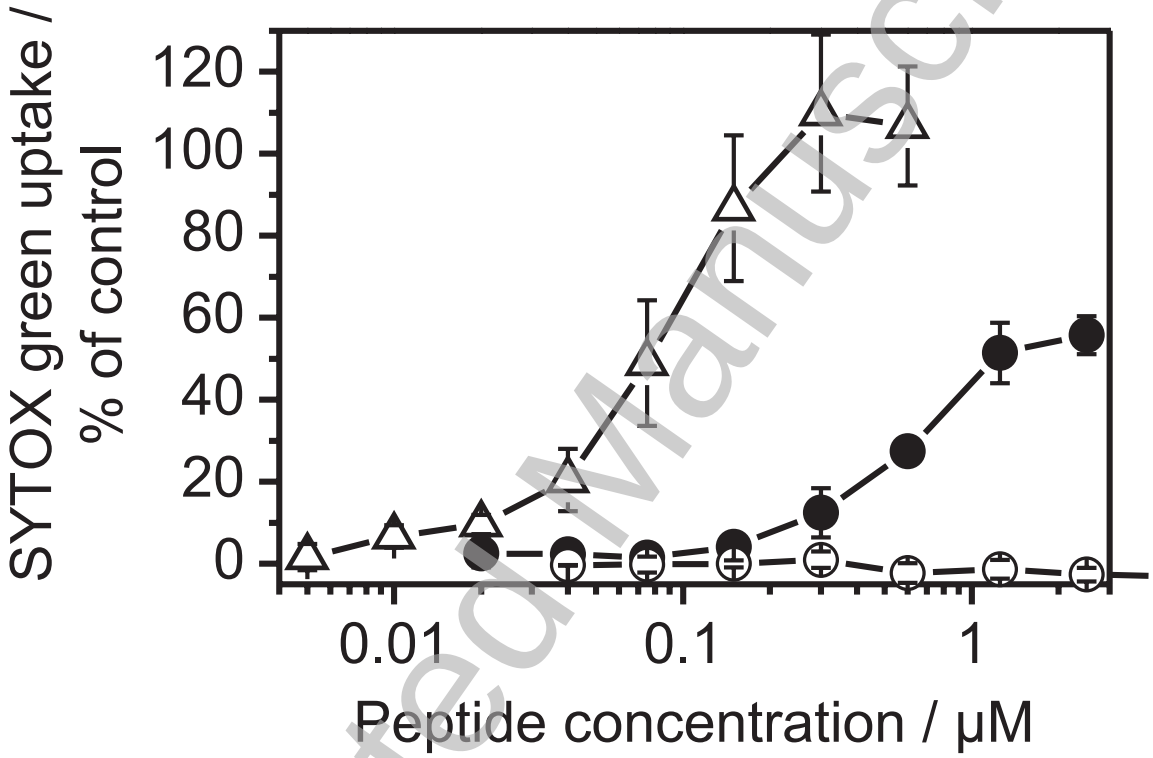

Biochemical Journal Immediate Publication. Published on 26 Feb 2010 as manuscript BJ20091607

Figure 7

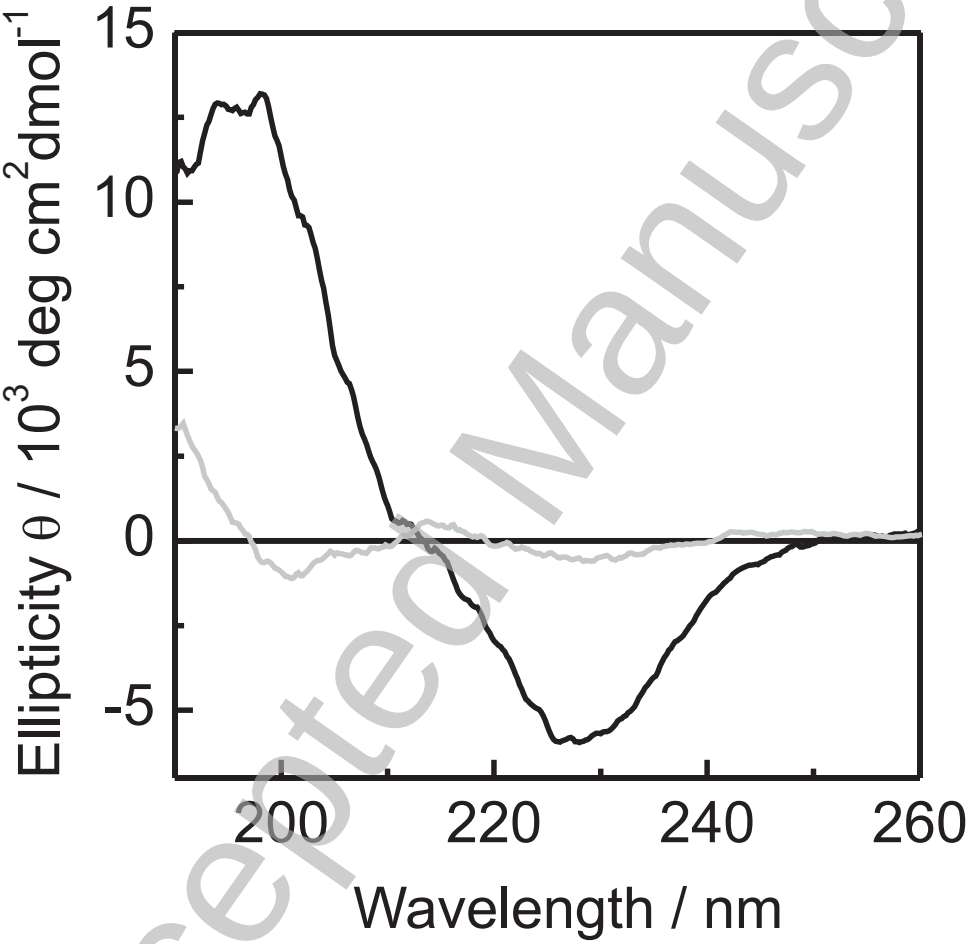

Biochemical Journal Immediate Publication. Published on 26 Feb 2010 as manuscript BJ20091607

Figure 8

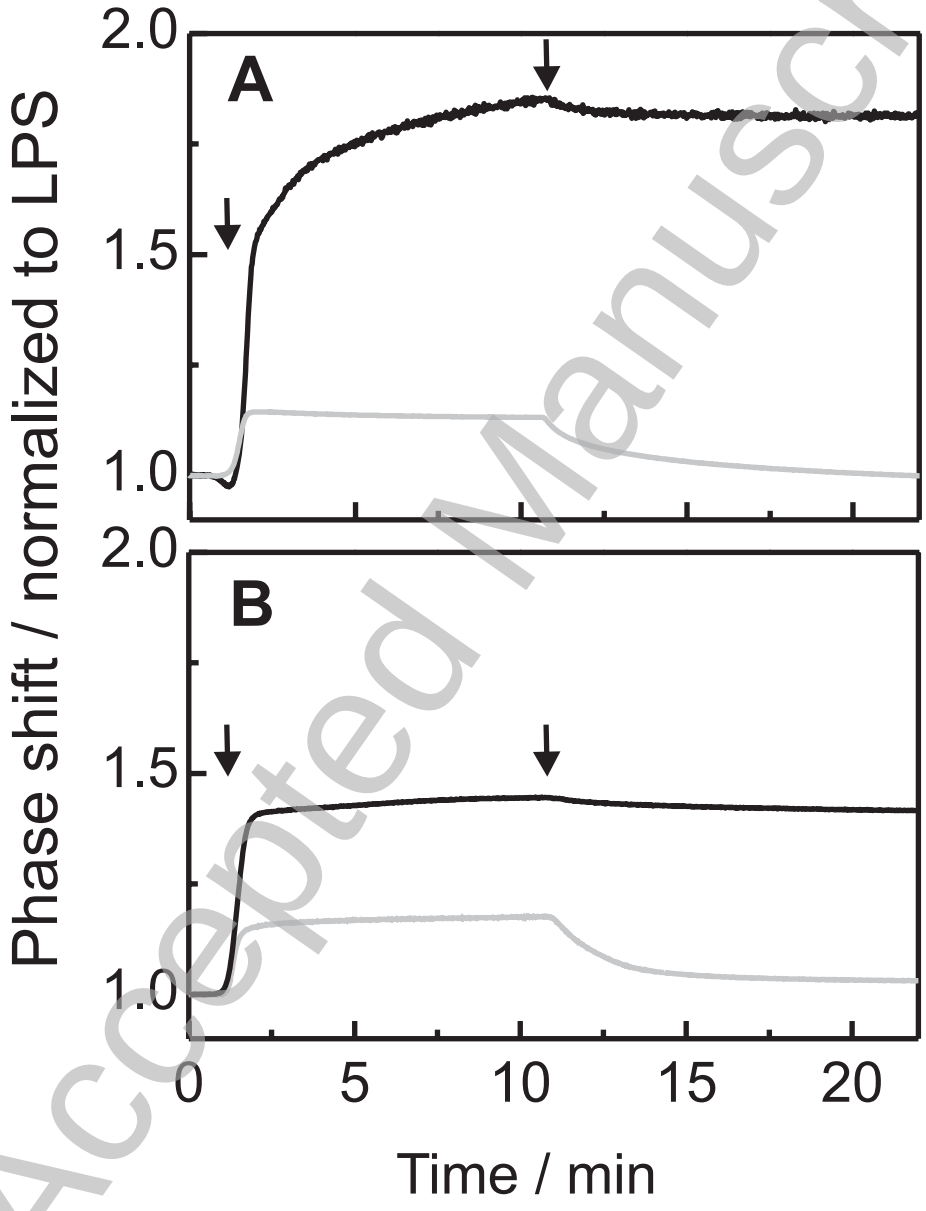

Biochemical Journal Immediate Publication. Published on 26 Feb 2010 as manuscript BJ20091607

Figure 9

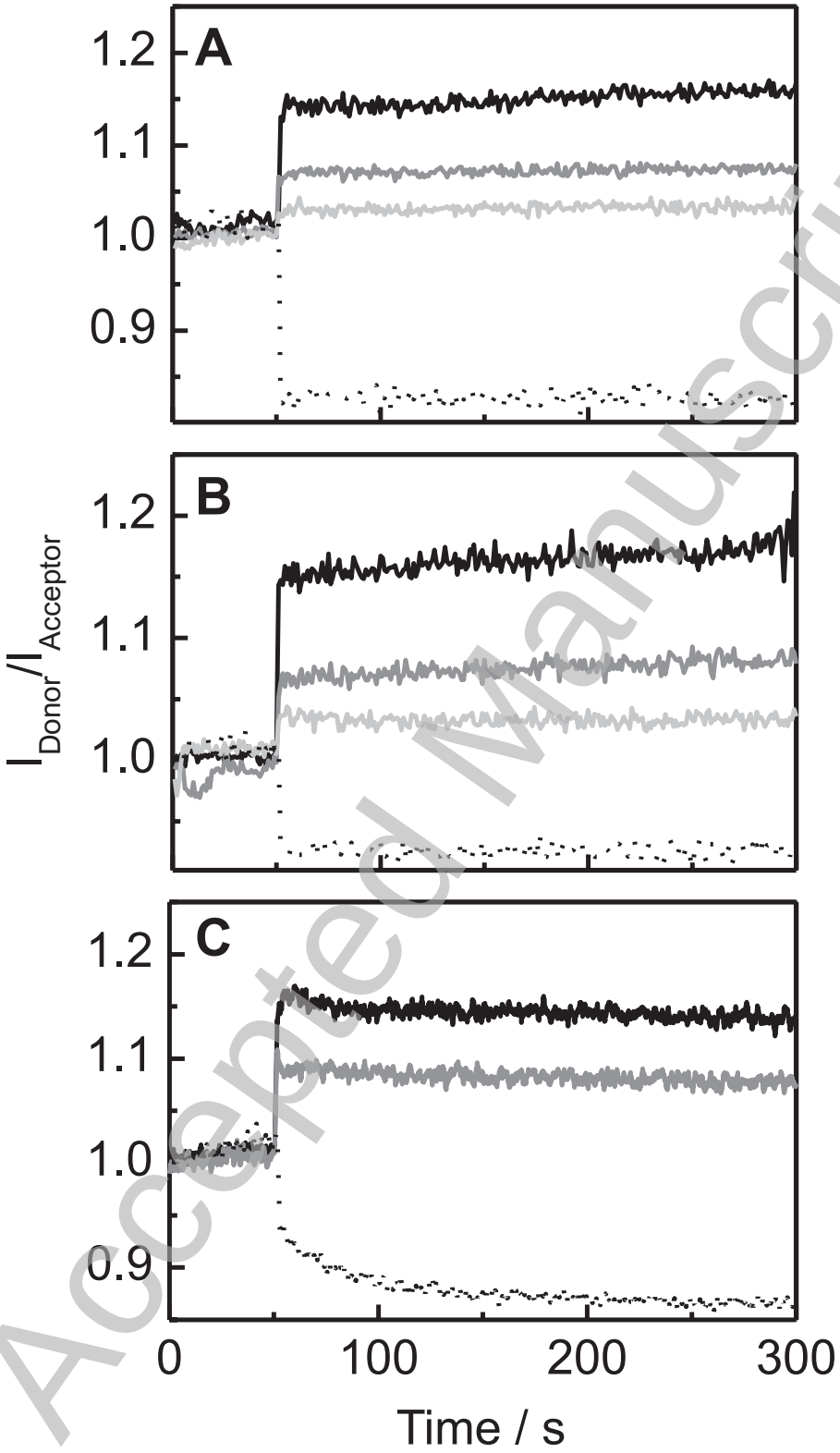

Biochemical Journal Immediate Publication. Published on 26 Feb 2010 as manuscript BJ20091607

Figure 10

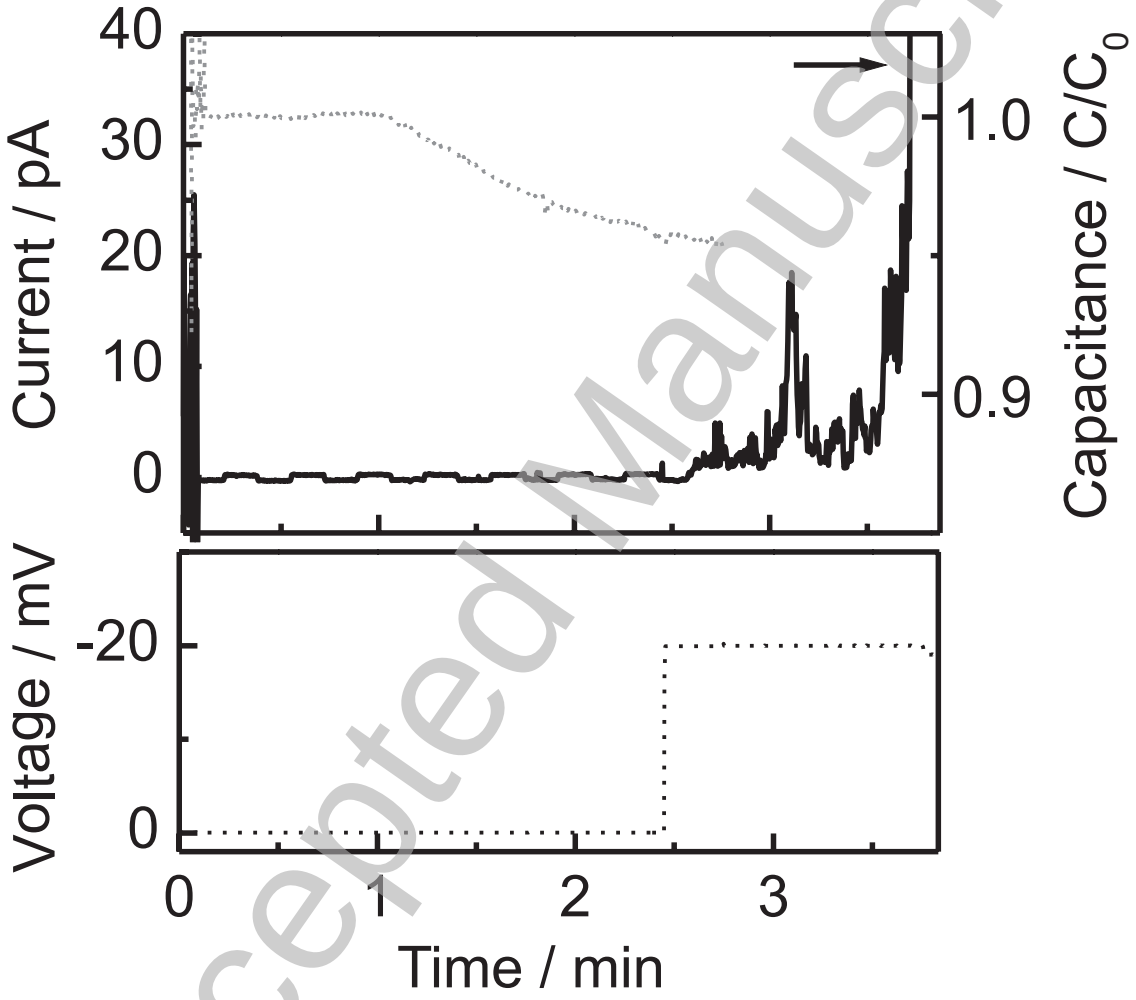

Figure 11

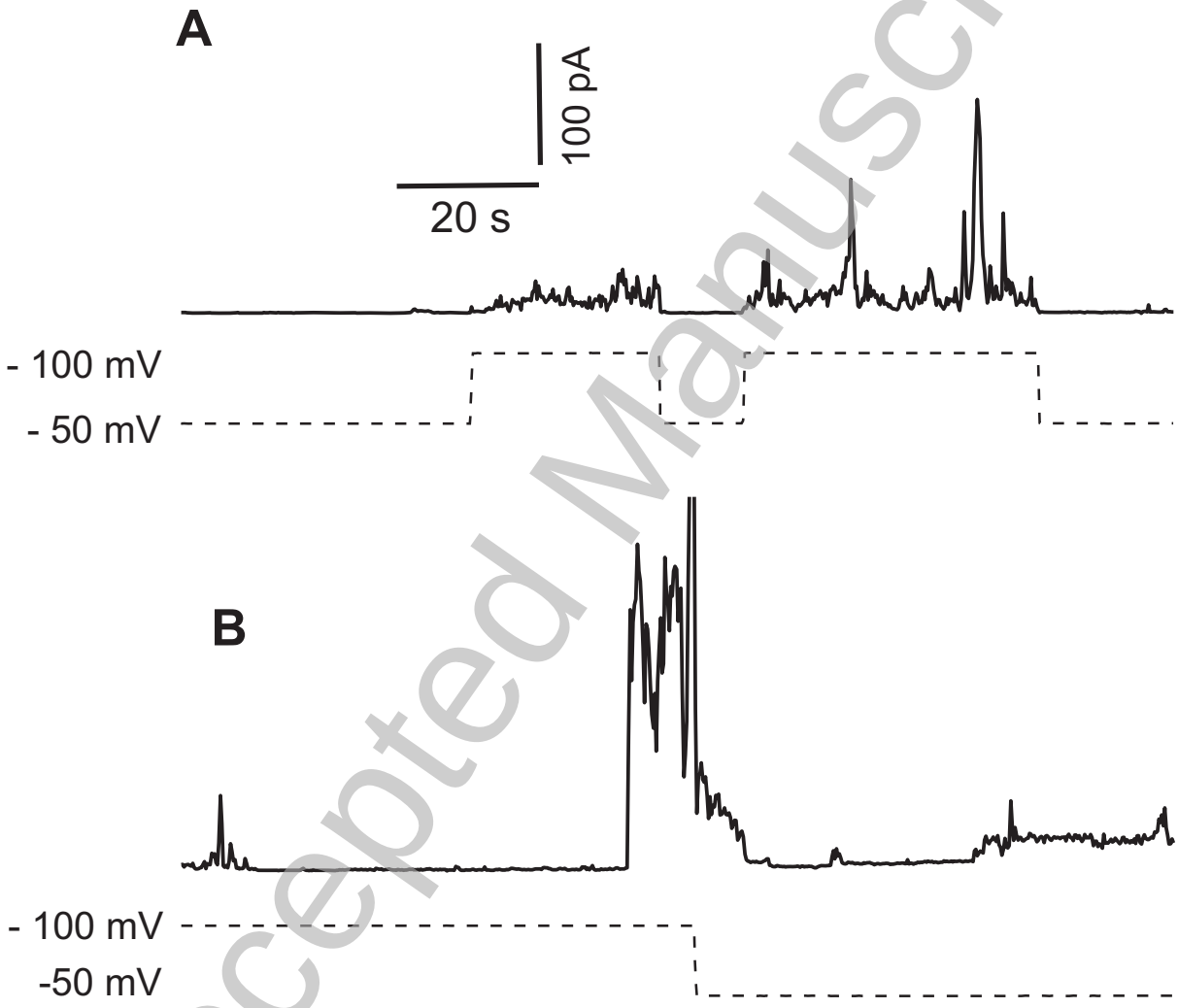

Biochemical Journal Immediate Publication. Published on 26 Feb 2010 as manuscript BJ20091607

Figure 12